Multicopy plasmids are clustered and localized in *Escherichia coli*

Joe Pogliano, Thanh Quoc Ho, Zhenping Zhong, and Donald R. Helinski*

Division of Biology, University of California at San Diego, 9500 Gilman Drive, La Jolla, CA 92130-0322

Contributed by Donald R. Helinski, February 14, 2001

We localized the multicopy plasmid RK2 in *Escherichia coli* and found that the number of fluorescent foci observed in each cell was substantially less than the copy number of the plasmid, suggesting that many copies of RK2 are grouped into a few multiplasmid clusters. In minimal glucose media, the majority of cells had one or two foci, with a single focus localized near midcell, and two foci near the 1/4 and 3/4 cell positions. The number of foci per cell increased with cell length and with growth rate, and decreased upon entering stationary phase, suggesting a coordination of RK2 replication or segregation with the bacterial cell cycle. Time-lapse microscopy demonstrated that partitioning of RK2 foci is achieved by the splitting of a single focus into two or three smaller foci, which are capable of separating with rapid kinetics. A derivative of the high-copy-number plasmid pUC19 containing the *lacO* array was also localized by tagging with GFP-LacI. Whereas many of the cells contained numerous, randomly diffusing foci, most cells exhibited one or two plasmid clusters located at midcell or the cell quarter positions. Our results suggest a model in which multicopy plasmids are not always randomly diffusing throughout the cell as previously thought, but can be replicated and partitioned in clusters targeted to specific locations.

The assumption that multicopy plasmids are free to diffuse randomly throughout the cell has been a generally accepted concept in plasmid biology for over two decades. Most models for multicopy plasmid replication and partitioning incorporate this concept as one of their underlying basic assumptions. For example, high-copy-number plasmids such as ColE1 and derivatives such as pUC19 (present at 30–200 copies per cell depending on the particular plasmid, strain, and growth temperature), are believed to rely entirely on random diffusion for inheritance into daughter cells (1, 2). Consistent with this idea, ColE1 plasmids do not encode active partitioning mechanisms. As another example, replication of the multicopy plasmid RK2 (present at five to eight copies per chromosome) is thought to be controlled by the intracellular plasmid concentration, which decreases when cell growth occurs in the absence of plasmid replication (3, 4).

Very low-copy-number plasmids (present at one to a few copies per chromosome), such as F, P1, and R1, have been localized in *Escherichia coli* (1, 5–9). For visualization of plasmid molecules in living cells, F and P1 were tagged with an array of *lacO* operator sequences containing the binding site for the LacI repressor repeated in tandem ≈256 times. F and P1 were detected by simultaneously expressing a green fluorescent protein (GFP)-LacI fusion protein from a compatible plasmid (8). For visualization in fixed cells, plasmid F was localized by using fluorescence *in situ* hybridization (FISH; ref. 6). Both plasmids localize to the cell midpoint and migrate rapidly after duplication to the 1/4 and 3/4 cell positions, which become the midpoints of the daughter cells after cell division.

Localization of these plasmids is thought to be mediated by the partitioning (Par or Sop) systems they encode because (*i*) the ParB protein of P1 shows a pattern of localization that depends on the *parS* DNA binding site and is similar to that reported for the P1 plasmid (10); (*ii*) miniF plasmids lacking the *sopAB* partitioning genes are more randomly distributed in the cell (6); and (*iii*) in the absence of a Par system, the P1 and F plasmids are rapidly lost from the population (9, 11). One emerging model is that these Par systems prevent the otherwise normal tendency of plasmids to be randomly distributed by directing newly duplicated plasmids to specific subcellular regions (midcell and cell quarter).

Recent studies show that DNA replication occurs in stationary factories located near the midcell or cell quarter positions in both *Bacillus subtilis* (12, 13) and *E. coli* (14–18). If multicopy plasmids randomly diffuse throughout the cell, but DNA replication occurs in stationary factories, how is replication of multicopy plasmids *in vivo* achieved? To gain insight into the mechanisms of replication and partitioning of multicopy plasmids, we localized RK2 in *E. coli* by using both GFP-LacI tagging and FISH, and we localized a derivative of the high-copy-number plasmid pUC19 by using GFP-LacI. We show that these two multicopy plasmids can be targeted to specific subcellular locations, notably at midcell or cell quarter positions, similar to those reported for low-copy-number plasmids and DNA replication proteins.

Materials and Methods

Strains, Media, and Growth Conditions. Plasmids were introduced into the *E. coli* strain JP313 (19) or DH5α (Life Technologies, Grand Island, NY) to create JP704 (JP313/RK2), JP872 (JP313/pZZ6/pGAP60), JP873 (JP313/RK2/pGAP60), JP839 (JP313/pAFS52/pGAP60), JP892 (JP313/pUC19/pGAP60), JP760 (DH5α/p52–1), JP765 (DH5α/pAFS52Δ1/p52–1), and JP787 (DH5α/p52–1/pUC19). Strain SM10 contains an RK2 plasmid integrated into the chromosome (20). Strains were grown in M63/0.2% glucose or LB. pGAP18 was constructed by using PCR to amplify the *gfpmut2* gene from pMut2 (21) using the primers 5′-TCATCTAGATTTAAGAAGGAG-3′ and 5′-GATTCTAGATTTGTATAGTTCATC-3′ and ligating the *Xba*I-digested PCR product with *Xba*I-digested pBAD33 (22). Plasmid pALH4 expresses GFPmut2 constitutively from the P*neo* promoter from Tn*5*; it was constructed by amplifying with PCR a 0.3-kb region of DNA containing the P*neo* promoter from plasmid pRR10 (23) using the primers 5′-CAGGGTACCTC-CGTCAGCTTCACGCTGC-3′ and 5′-CAGGGTACCGCGC-CATCAGATCCTTGG-3′. The *Kpn*I-digested product was ligated to *Kpn*I-digested pGAP18 DNA. Plasmid p52–1 expresses GFP-LacI constitutively from the P*neo* promoter of Tn*5* and was constructed by cloning the *Pml*I–*Nhe*I fragment from pSG20 (8) into the same sites of plasmid pALH4. Plasmid pGAP60 contains the GFP-LacI gene expressed from the arabinose promoter and a pACYC184 origin of replication; pGAP60 was constructed by deleting the P*neo* promoter from p52–1 by digestion with

Abbreviations: FISH, fluorescence *in situ* hybridization; GFP, green fluorescent protein; DAPI, 4′,6-diamidino-2-phenylindole.

*To whom reprint request should be addressed at: Bonner Hall 3401, University of California at San Diego, 9500 Gilman Drive, La Jolla, CA 92130-0322. E-mail: helinski@biomail.ucsd.edu.

The publication costs of this article were defrayed in part by page charge payment. This article must therefore be hereby marked "*advertisement*" in accordance with 18 U.S.C. §1734 solely to indicate this fact.

www.pnas.org/cgi/doi/10.1073/pnas.081075798

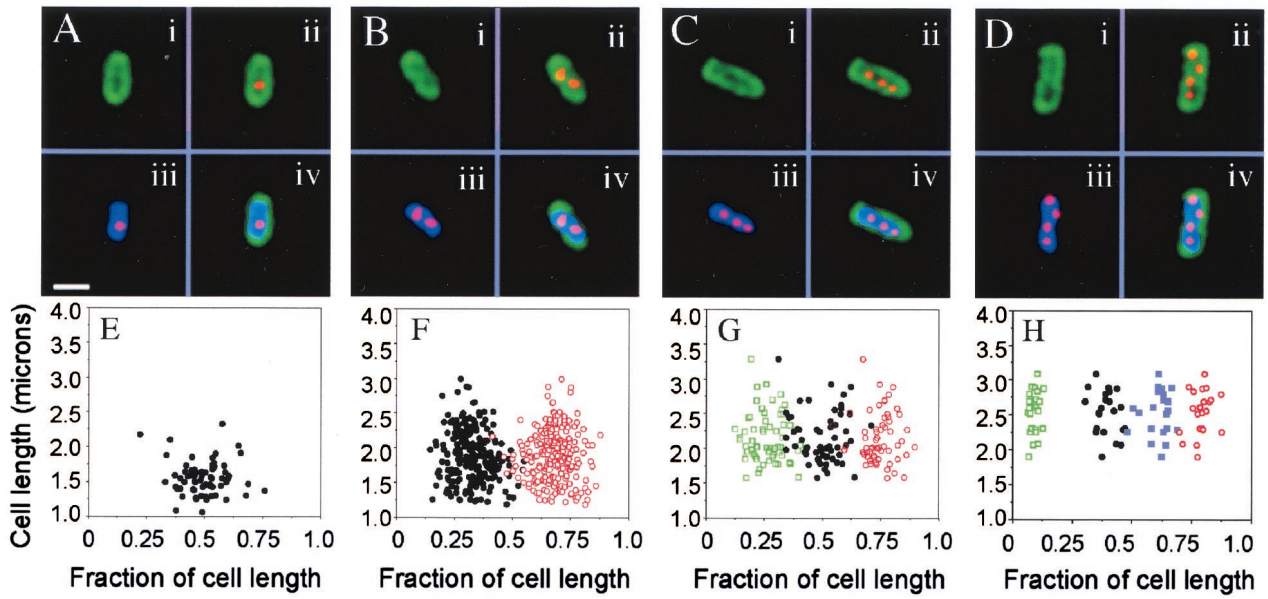

Fig. 1. Subcellular localization of RK2 in *E. coli* by FISH. (*A–D*) Strain JP704 was grown in M63/glucose at 37°C, fixed with paraformaldehyde, and hybridized with a Cy3-labeled RK2 probe. RK2 foci are red (*ii*, *iii*, and *iv*), the cell membranes are green because of staining with Mitotracker Green FM (*i*, *ii*, and *iv*), and DNA is stained with DAPI (*iii* and *iv*). Fluorescence micrographs of representative cells containing one focus (*A*), two foci (*B*), three foci (*C*), and four foci (*D*). (Bar = 1 μm.) (*E–H*) Subcellular distribution of RK2 in strain JP704 grown in M63/glucose at 37°C as determined by FISH. The position of each focus was measured with respect to one end of the cell. Cell length (in microns) is plotted against position of foci (given as a fraction of cell length). A total of 373 cells were measured. Graphs contain data for cells containing one (*E*, 18%), two (*F*, 60%), three (*G*, 14%), and four (*H*, 6%) foci.

*Kpn*I, followed by self-ligation. Plasmid pAFS52 (24) contains the 10-kb *lacO* array and the pUC19 origin of replication from pYIplac204 (25). Plasmid pZZ6 is an RK2 derivative containing the *lacO* array; pZZ6 was constructed by ligating the 10-kb *Sma*I–*Hin*dIII fragment of pAFS52 containing the *lacO* array to the 57.8-kb *Hpa*I–*Hin*dIII fragment of RK2. Chloramphenicol (10 μg/ml) was used to select for pACYC plasmids, ampicillin (50 μg/ml) was used for RK2 plasmids, and ampicillin (100 μg/ml) was used for pUC19 plasmids.

Preparation of Probes. Probes for FISH were prepared as described (26). Briefly, RK2 DNA (20 μg) was digested with six enzymes (*Alu*I, *Hae*III, *Mse*I, *Msp*I, *Rsa*I, and *Sau*3AI) to produce fragments ranging in size from 20 to 300 base pairs and labeled with Cy3-dCTP by terminal deoxynucleotidyltransferase (Promega).

FISH. FISH was performed as described by Jensen and Shapiro (27). Samples (0.5 ml) of exponentially growing cultures (2×10^8 cells per ml) were fixed for 10 min with 2.6% paraformaldehyde/32 mM phosphate buffer for LB or 1.4% paraformaldehyde/32 mM phosphate buffer for M63/glucose. Fixed cells were washed three times with PBS and resuspended in 200 μl of GTE (50 mM glucose/10 mM EDTA/20 mM Tris, pH 7.5). Samples of 10 μl were affixed to poly-L-lysine-treated wells of a multiwell slide and allowed to air dry. Blocking solution (1 mg/ml salmon sperm DNA/70% formamide/2× SSC) was added to each well, and the slide was heated to 75°C for 2 min and then transferred to 70%, 90%, and 100% ethanol baths for 5 min each. After air drying, 10 μl of 50% formamide/2× SSC solution was added for 5 min and then removed by aspiration, and 10 μl of probe solution (200 ng/μl) was added to each well. The slide was heated at 94°C for 2 min and incubated at 42°C for 1 h. The slide was washed twice in 10 μl of 50% formamide/2× SSC at 42°C for 30 min, once in 10 μl of 50% formamide/2× SSC at room temperature for 10 min, three times in 10 μl of 2× SSC at room temperature for 10 min, and twice quickly in PBS. Cells were stained with 0.5 μg/ml 4′,6-diamidino-2-phenylindole (DAPI)/0.2 μg/ml Mitotracker Green FM (Molecular Probes) and mounted in SlowFade/10% glycerol/PBS (Molecular Probes).

***In Vivo* Visualization of GFP-LacI-Tagged Plasmids.** In LB, strains containing the plasmid pGAP60 (GFP-LacI) and either pZZ6 (JP872) or RK2 (JP873) were grown overnight in LB at 23°C or at 30°C, diluted 1/100 in fresh media, and grown until OD_{600} = 0.1. GFP-LacI was induced for 20 min with 0.2% L-arabinose, and then repressed with 0.2% glucose to prevent overexpression. After 2.5 to 3 h of growth ($0.4 \leq OD_{600} \leq 0.6$), cells were stained with 1 μg/ml FM 4–64 and 5 μg/ml DAPI, and then affixed to a poly-L-lysine-treated coverslip. GFP-LacI was induced in M63/glucose by the addition of 0.2% L-arabinose; samples were collected 3 h later and stained with 0.1 μg/ml FM 4–64 and 5 μg/ml DAPI. Images from six optical sections spaced 0.15 μm apart were captured with an Applied Precision Deconvolution microscope as described (28). All images presented were deconvolved by using DELTAVISION V2.1 software. For quantitation of the number and position of foci, six optical sections were scanned to ensure that all foci in each cell were counted. For time-lapse microscopy, cells were grown with FM 4–64 (0.2 μg/ml) and concentrated 10-fold by centrifugation, and 10 μl was placed on an agarose slab (0.9% agarose/1% LB/0.2% glucose). The microscope objective and agarose pad were heated to 30°C, and images of cells were captured at the times indicated. While under observation, cells grew with a doubling time of 40 min.

Results and Discussion

Localization of RK2 in Fixed Cells by Using FISH. We localized RK2 in the *E. coli* strain JP704 grown in M63/glucose at 37°C by FISH (Fig. 1 *A–D*). RK2 was detected by using Cy3-labeled RK2 DNA (red foci); the DNA was stained with DAPI (blue), and the cell membranes were stained with Mitotracker Green FM (green). In 18% of cells, only one focus was observed; in 60% of cells, two RK2 foci were observed (Fig. 1 *A* and *B*). Less frequently, three

(14%) and four (6%) foci per cell were seen (Fig. 1 *C* and *D*). None of the cells contained more than four foci, whereas 2% did not show any foci. In control strains without RK2, no foci were seen (data not shown). In strains containing RK2 integrated into the chromosome (SM10), we were able to detect one or two fluorescent foci per nucleoid, demonstrating that our technique is sensitive enough to detect a single copy of RK2 (data not shown).

The positions of RK2 foci varied depending on the total number in each cell. In Fig. 1 *E–H*, the position of each focus is plotted against fraction of cell length. A single focus was located preferentially near midcell, whereas two foci were located preferentially near the 1/4 and 3/4 cell positions (Fig. 1 *E* and *F*). When three foci were present, one focus was often located near midcell and the other two were located near the 1/4 and 3/4 cell positions (Fig. 1*G*). In cells containing four foci, the foci were found approximately at the 1/8, 3/8, 5/8, and 7/8 cell positions (Fig. 1*H*). In addition, the pattern of localization showed a strong correlation with cell length, which is an approximate indicator of progression through the cell cycle in *E. coli* (29). The average length for cells containing one, two, three, and four foci was 1.5 μm, 1.9 μm, 2.1 μm, and 2.5 μm, respectively (Fig. 1 *E–H*). Furthermore, 90% of the cells containing one focus were less than 2 μm in length, whereas 95% of cells containing four foci were greater than 2 μm in length (Fig. 1 *E* and *H*). This finding suggests that the shorter, newborn cells have a single focus at midcell that duplicates into two foci, which then migrate to the cell quarter positions.

Localization of RK2 in Live Cells. Fixation with paraformaldehyde and other manipulations during FISH experiments could potentially affect or alter plasmid localization. To independently confirm results obtained from FISH experiments, RK2 was localized in living cells by GFP-LacI tagging (8, 30). A DNA cassette containing the *lacO* array was inserted into the wild-type 60-kb RK2 plasmid to create plasmid pZZ6 (RK2-*lacO*). The RK2-*lacO* plasmid was detected by expressing a GFP-LacI fusion protein from the arabinose promoter on the compatible plasmid pGAP60.

Strains containing pGAP60 and either RK2-*lacO* or RK2 were grown in M63/glucose at 23°C; GFP-LacI expression was induced by the addition of 0.2% L-arabinose. Approximately 3 h later (OD_{600} = 0.5), samples were stained with FM 4–64 to visualize the cell membranes (red) and with DAPI to visualize the nucleoids (blue; Fig. 2). Upon induction of GFP-LacI, green fluorescence filled the cytoplasm of the control strain containing wild-type RK2 without the *lacO* array (Fig. 2 *D–F*). In contrast, green fluorescent foci appeared in 99% of the cells containing RK2-*lacO* (Fig. 2 *A–C*). Whereas GFP-LacI often forms inclusion bodies when expressed from high-copy-number plasmids (such as pUC19) at 30°C (8), it does not produce inclusion bodies (or fluorescent foci in strains without the *lacO* array) when expressed from plasmid pGAP60 (a pACYC184 derivative) at 30°C. Nonetheless, to ensure that temperature did not affect our results, we performed all localization experiments at both 23°C and 30°C and obtained similar results at each temperature. We quantitated the number and positions of GFP foci and plotted the position of foci against fraction of cell length (Fig. 3 *A* and *B*). Most cells contained either a single focus (39%) located preferentially near the cell midpoint (Fig. 3*A*), or two foci (46%) near the 1/4 and 3/4 cell positions (Fig. 3*B*). Cells containing three, four, and five foci comprised 8%, 4%, and 2% of the population, respectively, whereas 1% of cells lacked foci (data not shown). These results agree well with those obtained by using FISH.

Our results demonstrate that RK2 is not randomly positioned in the cell, but rather is localized to the cell midpoints or future midpoints, similar to the very low-copy-number plasmids F and P1. This finding suggests that several different plasmids are targeted to the same general location in *E. coli*. Like plasmid F, the position of RK2 varied with cell length, suggesting that duplication or segregation is coordinated with the cell division cycle. The pattern of RK2 localization is also strikingly similar to that reported for the RK2-encoded partitioning protein KorB (31).

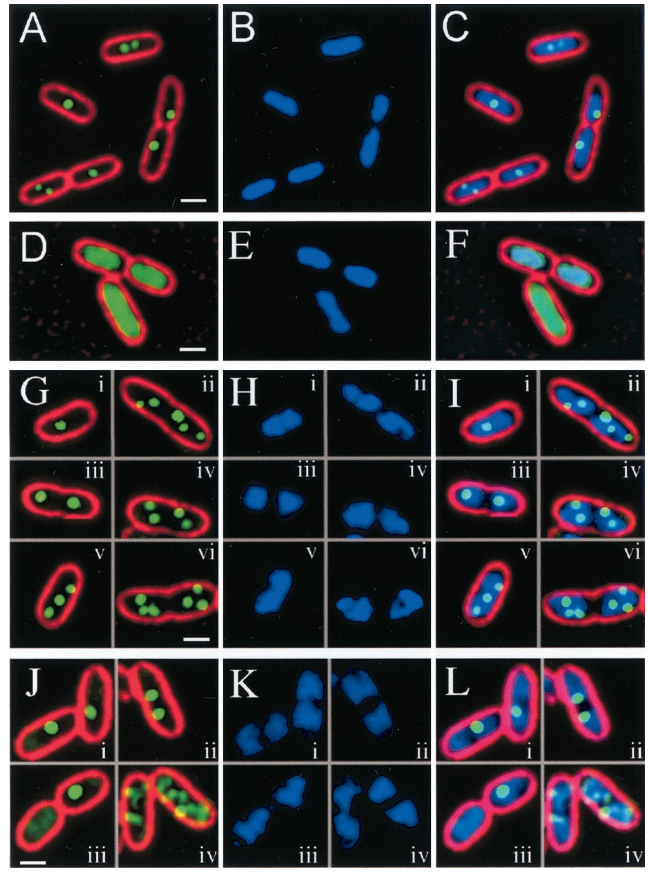

Fig. 2. Localization of RK2-*lacO* (pZZ6) and pUC19-*lacO* (pAFS52) plasmids by tagging with GFP-LacI at 23°C. GFP-LacI was expressed from plasmid pGAP60 by induction with 0.2% L-arabinose, as described in *Materials and Methods*. Cell membranes were stained with FM 4–64 (red), DNA was stained with DAPI (blue), and GFP-tagged plasmids appear as green foci. (*A–C*) Strain JP872 (containing RK2-*lacO*) grown in M63/glucose. (*D–F*) Strain JP873 (containing RK2) grown in M63/glucose. (*G–I*) Strain JP872 (containing RK2-*lacO*) grown in LB/glucose, showing cells containing one (*i*), two (*iii*), three (*v*), four (*iv*), five (*ii*), and six (*vi*) foci. (*J–L*) Strain JP839 containing the pUC-*lacO* derivative pAFS52 grown in LB/glucose, showing cells containing one (*i*) and two (*ii*) foci, a cell nearly finished dividing (*iii*), and cells with multiple foci (*iv*). (Bars = 1 μm.)

Effect of Growth Rate on RK2 Localization. To determine whether RK2 localization is influenced by growth rate, we compared the number of foci per cell in strains grown in M63/glucose to the number per cell in strains grown in LB/glucose. Strains (JP872 and JP873) were grown in LB at 23°C, and GFP-LacI expression was induced with 0.2% L-arabinose. After 20 min, further expression of GFP-LacI was inhibited by the addition of 0.2% glucose and samples were collected for microscopy ≈2.5 h later (OD_{600} = 0.5). No fluorescent foci were observed after arabinose induction in the strain (JP873) containing the wild-type RK2 plasmid without the *lacO* array (data not shown). In the strain (JP872) containing RK2-*lacO*, we observed up to 10 foci per cell in LB/glucose at 23°C (Fig. 2 *G–I* and Fig. 4*A*, blue bars). More than 80% of the cells had three or more foci, with four

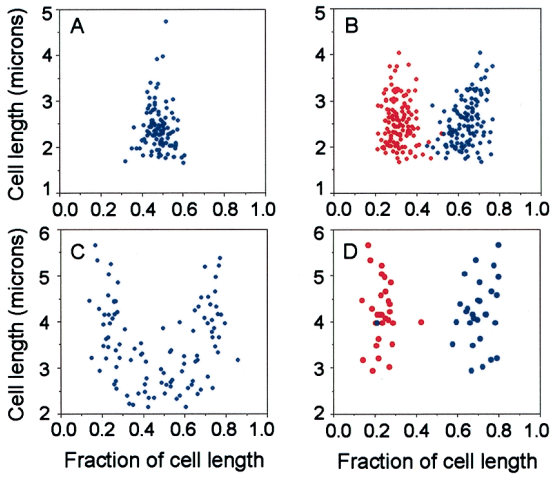

Fig. 3. Subcellular distribution of GFP-tagged pZZ6 (RK2-*lacO*) and pAFS52 (pUC-*lacO*) in *E. coli*. Cell length (in microns) is plotted against position of GFP foci (given as a fraction of cell length). (*A* and *B*) Strain JP872 containing RK2-*lacO* was grown in M63/glucose at 30°C. A total of 282 cells were measured; 39% had a single focus (*A*), 46% had two foci (*B*), and 8%, 4%, and 2% had three, four, and five foci, respectively (data not shown). (*C* and *D*) Strain JP839 containing plasmid pAFS52 was grown in LB/glucose at 23°C. A total of 124 cells were measured; 99 cells contained one focus (*C*) and 25 cells contained two foci (*D*).

(30%) and five foci (24%) constituting the two largest classes. In minimal glucose media, on the other hand, more than 80% of the cells contained only one or two foci (Fig. 4*A*, yellow bars). Nearly identical results were obtained when strains were grown at 30°C (data not shown). We independently confirmed these results by localizing RK2 in strain JP704 grown in LB at 30°C by FISH and obtained similar results (Fig. 4*B*).

We also explored the effect of growth phase on foci number by quantitating RK2 localization in a culture during exponential growth in LB/glucose at 23°C and after the same culture had transitioned to stationary phase. The number of foci per cell during exponential growth from Fig. 4*A* is replotted in Fig. 4*C* (note different *y*-axis scale) and compared with the number of foci per cell ≈1.5 h after entry into stationary phase (OD_{600} = 3.5). Although 80% of the exponential-phase cells contained three or more foci (Fig. 4*C*, dark blue bars), 76% contained less than three foci after entering stationary phase, with the largest class (37%) containing a single focus (Fig. 4*C*, light blue bars).

The number of RK2 foci per cell is dramatically affected by both the growth media and the growth phase, in a manner similar to that seen for fusions of SeqA to GFP in *E. coli* (16, 17) and PolC-GFP in *B. subtilis* (12). In these cases, the higher number of foci during more rapid growth reflects the increased number of replication forks per cell. This similarity in RK2 and SeqA localization suggests that the number and position of RK2 foci may also reflect the number and position of chromosomal DNA replication forks. Alternatively, plasmid and chromosome replication may be similarly regulated.

RK2 Plasmids Form Clusters. Several different methods of plasmid-copy-number determination have established that RK2 is present at five to eight copies per chromosome (32–37); therefore, we expected ≈5–10 foci in slowly growing cells, and 10–20 foci in rapidly growing cells. Instead, 90% of the cells grown in LB/glucose at 23°C (Fig. 2 *G–I* and Fig. 4*A*) or LB at 30°C (Fig. 4*B*) contained between two and six foci. We conclude that the number of foci per cell does not correspond to the number of plasmids per cell, indicating that each focus consists of more than one plasmid. Multimer formation is not likely to explain this clustering effect, because RK2 encodes a potent multimer-resolution system and is maintained primarily as monomers within the cell (38, 39). The unrelated plasmid R1 also exists as clusters in *E. coli* (40), suggesting that formation of multiplasmid bundles may be a feature common to many plasmids.

Visualization of RK2 Segregation. Time-lapse microscopy experiments allowed us to observe RK2-*lacO* segregation *in vivo*. Cells containing GFP-tagged RK2-*lacO* were stained with FM 4–64, placed on an agarose slab, and heated to 30°C; images were captured at various time intervals. Two examples of RK2-*lacO* segregation are shown in Fig. 5 *A* and *B*. When time points were 10 min apart, we could readily observe a single focus split into two foci (Fig. 5*A*). Duplication of foci frequently occurred at the cell quarter positions (Fig. 5*A*, top cell) in addition to occurring at midcell (data not shown). Two midcell foci were readily observed to migrate to the 1/4 and 3/4 cell positions (Fig. 5*A*, bottom cell).

To determine the rate of separation of RK2 foci, we performed time-lapse microscopy of GFP-tagged RK2-*lacO* at 30°C, and collected images 1 min apart. One example is shown in Fig. 5*B*. At time 0, the cell contains three foci that are very close together at midcell; by the 7-min time point, they resolve into three well separated foci. Between the 9- and 10-min time points, the top two foci separate more than 0.5 μm from the bottom focus.

For a few foci that showed duplication and separation, the distance between the foci was measured and plotted against time (Fig. 6). Some foci showed a dramatic jump in the separation distance between two time points, followed by a more gradual separation from each other (Fig. 6). Other foci showed relatively

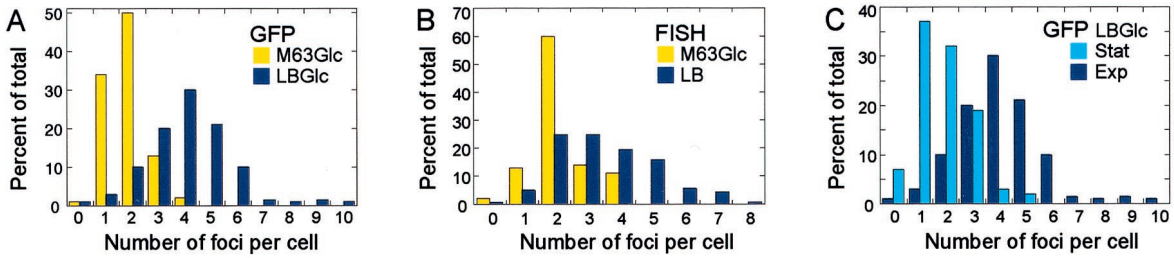

Fig. 4. Histograms showing the number of RK2 foci per cell in different growth conditions. Percentage of total cells is plotted against the number of foci per cell. (*A*) Number of GFP foci per cell in strain JP872 (containing RK2-*lacO*) grown in M63/glucose at 23°C (yellow bars = 140 total cells) and LB/glucose at 23°C (blue bars = 135 total cells). (*B*) Number of RK2 foci per cell from FISH analysis of JP704 grown in M63/glucose at 37°C (yellow bars = 373 total cells) and LB at 30°C (blue bars = 241 total cells). (*C*) Number of GFP foci per cell in strain JP872 (containing RK2-*lacO*) during exponential growth in LB/glucose at 23°C (dark blue bars represent the same data shown in *A*) and 1.5 h after the same culture had transitioned to stationary phase (light blue bars = 110 total cells). Note the different *y*-axis scales.

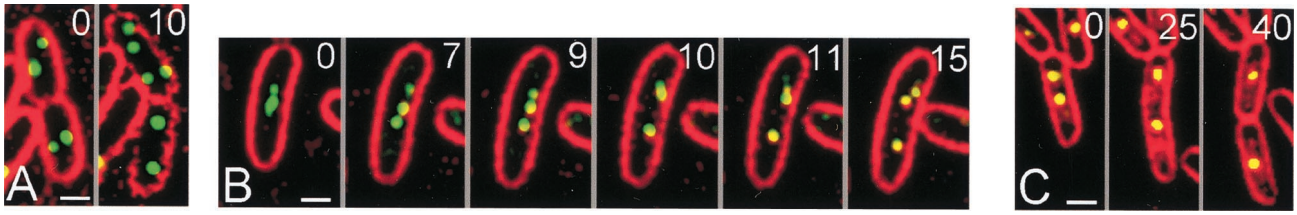

Fig. 5. Time-lapse microscopy of RK2-*lacO* and pUC-*lacO* segregation. Strains were grown in LB at 30°C, stained with FM 4–64 (red), and placed on an agarose slab; images were captured at various times by using a stage and microscope objective heated to 30°C as described in *Materials and Methods*. (Bars = 1 μm.) (*A*) Two time-lapse images taken 10 min apart of GFP-tagged RK2-*lacO* (JP872) showing the duplication of two foci into four foci (top cell) and the separation/migration of two midcell foci to the 1/4 and 3/4 cell positions (bottom cell). (*B*) Twenty images of JP872 (with GFP-tagged RK2-*lacO*) were collected 1 min apart; six of those images are shown. Three foci very close together at midcell at time 0 resolve into three clearly separate foci at midcell by the 7-min time point. Between the 9- and 10-min time points, the top two foci separate from the bottom focus more than 0.5 μm. Red shifting of GFP after repeated excitation yields foci that fluoresce both red and green, and therefore appear yellow when both colors are shown simultaneously. (*C*) Three time-lapse images of JP765 showing segregation of pUC-*lacO*. Two foci in one cell at time 0 migrate to the future midpoints of the two daughter cells by the 40-min time point.

gradual separation during the experiment (Fig. 6*B*, open circles). Many foci appeared to vibrate in three dimensions within the cell, accounting for the variation in the distance between foci over time (Fig. 6*A*, filled green circles). These experiments suggest that active partitioning of RK2 foci is achieved by the splitting of a single cluster of plasmids into two or three clusters, which then migrate in opposite directions from midcell to the cell quarter positions. Foci migration appears slow during most of the division cycle but is punctuated by periods of very rapid movement, with maximal rates (0.3 μm/min average for $n = 3$) similar to those reported for chromosome movement in *B. subtilis* (41) and SeqA migration in *E. coli* (15).

Localization of a High-Copy-Number Plasmid. The results described above suggested that multicopy plasmids may occur in clusters tethered near the cell midpoints or future midpoints, rather than existing as freely diffusable units. To address whether this was a property common to many multicopy plasmids or specific to RK2, we localized the plasmid pAFS52 (24), which contains the 10-kb *lacO* array and an origin of replication derived from pUC19 (25). The copy number of pUC19 and its derivatives varies from 40 to 250 copies per cell depending on the host strain and temperature (42). In our particular growth conditions, quantitation of pAFS52 demonstrated that at least 70 copies per cell were present before and after GFP-LacI expression (data not shown).

Strains JP839 (containing pAFS52) and JP892 (containing pUC19) were grown in LB at 23°C; GFP-LacI was induced with 0.2% L-arabinose from the compatible plasmid pGAP60. After 20 min, further expression of GFP-LacI was inhibited by the addition of 0.2% glucose. Under these conditions, whole-cell green fluorescence of GFP-LacI was always observed in strains

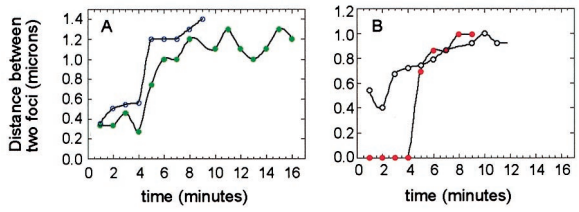

Fig. 6. Rate of separation of GFP-tagged RK2-*lacO* plasmids. Time-lapse microscopy of strain JP872 grown in LB/glucose at 30°C was performed as described in *Materials and Methods*. Images were collected 1 min apart, and the distance between foci was measured and plotted against time (min). (*A*) Two foci showing rapid separation over a 1-min (open blue circles) or 2-min (filled green circles) time interval. (*B*) Two foci showing gradual separation (open circles) and duplication of a single focus into two foci which then separate more than 0.7 μm over a 1-min time interval (filled red circles).

containing pUC19. Surprisingly, in strains containing pAFS52, we observed two distinct patterns of localization. First, 90% of the cells contained one or two bright foci, suggesting that many of the plasmid copies in the cell were grouped into one or two large clusters (Fig. 2*J–L*). Second, many cells (≈30%), including some of those containing bright foci, appeared to have plasmids randomly diffusing throughout the cytoplasm (Fig. 2*Jiv*). These foci were faint, rapidly moving, and difficult to capture in photographic images.

We measured the lengths of the cells and the positions of bright GFP foci for a culture growing exponentially in LB/glucose at 23°C. A single focus occurred preferentially near midcell or near one of the cell quarter positions (Fig. 3*C*). Localization near midcell generally occurred in the shorter cells, whereas localization near one of the cell quarter positions usually occurred in the longer cells. Less frequently (20%) two foci were observed that localized near the 1/4 and 3/4 cell positions (Fig. 3*D*). The localization pattern of two foci is similar to that for RK2. This tendency to cluster together could account for a significant amount of loss of the plasmid during growth. These results suggest the unexpected conclusion that high-copy-number plasmids are also targeted to specific positions during a portion of their replication cycle, as one or two large clusters.

To further explore this phenomenon, we localized pAFS52(Δ1), a spontaneous deletion derivative of pAFS52 containing only 1.5 kb of *lacO* repeat DNA, instead of 10 kb. GFP-LacI was expressed constitutively from the neomycin promoter of Tn*5* on the compatible plasmid p52–1. Despite having 85% less *lacO* repeat DNA on the plasmid, bright fluorescent foci located at midcell and cell quarter positions were observed in most cells of strain JP765 (DH5α/pAFS52(Δ1)/p52–1) but not in the control strains JP760 (DH5α/p52–1) or JP787 (DH5α/pUC19/p52–1; data not shown). Randomly diffusing foci were rarely observed in this strain. These results provide additional support for the proposal that multiple copies of this plasmid are clustered together.

Time-Lapse Microscopy of Active pUC Segregation. Although images of GFP-tagged pAFS52 suggested that high-copy-plasmids may exhibit localization patterns similar to RK2, F, and P1, it remained unclear how clusters of plasmids without a known partitioning system could be segregated. Therefore, we used time-lapse microscopy to observe movement and partitioning of GFP-tagged pAFS52(Δ1). Cells of JP765 were stained with FM 4–64, placed on an agarose slab, and heated to 30°C. We captured images of live cells every 5 min. As observed for RK2-*lacO*, pAFS52(Δ1) localization is dynamic. In Fig. 5*C*, two foci can be seen to migrate away from each other during cell growth, taking up positions at the 1/4 and 3/4 cell positions, so that each daughter cell inherits one focus. These results sug-

gested that the GFP-tagged pUC molecules may be actively partitioned, despite lacking a plasmid-encoded partitioning locus. Alternatively, pUC foci could dissociate into a pool of free molecules and later reform at different locations.

If the dynamic and complex nature of pAFS52 localization reported here reflects the *in vivo* situation for other ColE1-type plasmids, these results may reconcile the apparent incongruity of past studies, one of which indicated that pBR322 plasmids were clustered in the cell (43), and another which indicated that pBR322 plasmids were randomly localized (44). Both patterns of localization were observed.

Experiments to localize pUC19 by using FISH were inconclusive, and, therefore, we were unable to independently confirm these results. However, three lines of evidence suggest that the GFP-tagged foci observed *in vivo* are not inactive plasmid clusters, but may represent the normal dynamics of the plasmid. First, these clusters are located at midcell or at the 1/4 and 3/4 cell positions, similar to plasmids RK2, P1, and F; they are not randomly distributed in the cell or preferentially located in nucleoid-free zones where Par$^-$ miniF plasmids reside (6). Second, these foci appeared to migrate into daughter cells in time-lapse microscopy experiments. Third, plasmid replication (as determined by quantitation of plasmid DNA) was unaffected by the expression of GFP-LacI, as might be expected if these plasmids have aggregated artificially into inactive repositories. Finally, even if the clustering observed for pAFS52 were caused by GFP-LacI tagging, these results would still suggest that this plasmid is capable of targeting to the midcell and cell quarter positions. Dynamic targeting to these positions could be part of a mechanism for their DNA replication and partitioning (if they use a replisome fixed in these locations).

Models for Plasmid Replication and Partitioning. These results support a model in which clusters of plasmid copies are tethered to specific regions of the cell by as yet unidentified receptors, whose numbers and subcellular positions are closely regulated by the host-cell division cycle. As receptors duplicate and separate during cell growth, plasmid clusters are split apart and attach to the unoccupied receptors. The nature of these putative receptors is as yet unclear; however, there is a close correlation between the position and number of plasmid clusters and that of DNA-replication factories, suggesting that the receptor may be associated with, or a subunit of, the replication factories. Should this be the case, then plasmids could segregate by hitching a ride with the segregating DNA-replication machinery. Partitioning proteins may serve to regulate either the affinity of plasmids for the receptor, or their dynamic behavior during segregation. Those plasmids that lack a partitioning system (such as pUC19 or Par$^-$ mutants of F) may have a decreased affinity for, or unregulated binding to, these receptors, so that targeting is defective or transient and localization is more random. Regardless of the role of partitioning proteins in these processes, our results demonstrate that the ability of plasmids to localize within the bacterial cell is a feature of multicopy plasmids as well as single-copy plasmids, and that this feature is conserved even in small, high-copy-number plasmids such as pUC19.

We are grateful to Rasmus Jensen and Lucy Shapiro for providing the FISH protocol and to Scott Gordon and Andrew Wright for providing plasmids pSG20 and pAFS52. Aresa Toukdarian, Kit Pogliano, and Marc Sharp provided valuable discussions. This work was supported by a postdoctoral fellowship from the California Division of the American Cancer Society (to J.P.) and by the National Institutes of Health research Grant AI-07194.

1. Gordon, G. S. & Wright, A. (2000) *Annu. Rev. Microbiol.* **54,** 681–708.
2. del Solar, G. & Espinosa, M. (2000) *Mol. Microbiol.* **37,** 492–500.
3. Chattoraj, D. K. (2000) *Mol. Microbiol.* **37,** 467–476.
4. Helinski, D. R., Toukdarian, A. E. & Novick, R. P. (1996) in *Escherichia coli and Salmonella: Cellular and Molecular Biology*, ed. Neidhardt, F. C. (Am. Soc. Microbiol., Washington, DC), 2nd Ed., pp. 2295–2324.
5. Jensen, R. B. & Shapiro, L. (1999) *Curr. Opin. Cell Biol.* **11,** 726–731.
6. Niki, H. & Hiraga, S. (1997) *Cell* **90,** 951–957.
7. Weitao, T., Dasgupta, S. & Nordstrom, K. (2000) *Mol. Microbiol.* **38,** 392–400.
8. Gordon, G. S., Sitnikov, D., Webb, C. D., Teleman, A., Straight, A., Losick, R., Murray, A. W. & Wright, A. (1997) *Cell* **90,** 1113–1121.
9. Hiraga, S. (2000) *Annu. Rev. Genet.* **34,** 21–59.
10. Erdmann, N., Petroff, T. & Funnell, B. (1999) *Proc. Natl. Acad. Sci. USA* **96,** 14905–14910.
11. Nordstrom, K. & Austin, S. J. (1989) *Annu. Rev. Genet.* **23,** 37–69.
12. Lemmon, K. P. & Grossman, A. D. (1998) *Science* **282,** 1516–1519.
13. Lemmon, K. P. & Grossman, A. D. (2000) *Mol. Cell* **6,** 1321–1330.
14. Hiraga, S., Ichinose, C., Kiki, H. & Yamazoe, M. (1998) *Mol. Cell* **1,** 381–387.
15. Onogi, T., Niki, H., Yamazoe, M. & Hiraga, S. (1999) *Mol. Microbiol.* **31,** 1775–1782.
16. Hiraga, S., Ichinose, C., Onogi, T., Niki, H. & Yamazoe, M. (2000) *Genes Cells* **5,** 327–341.
17. Brendler, T., Sawitzke, J., Sergueev, K. & Austin, S. (2000) *EMBO J.* **19,** 6249–6258.
18. Koppes, L. J., Woldringh, C. L. & Nanninga, N. (1999) *Biochimie (Paris)* **81,** 803–810.
19. Economou, A., Pogliano, J. A., Beckwith, J., Oliver, D. B. & Wickner, W. (1995) *Cell* **83,** 1171–1181.
20. Simon, R., Priefer, U. & Puhler, A. (1983) in *Molecular Genetics of the Bacteria–Plant Interaction*, ed. Puhler, A. (Springer, Heidelberg), pp. 99–106.
21. Cormack, B. P., Valdivia, R. H. & Falkow, S. (1996) *Gene* **173,** 33–38.
22. Guzman, L. M., Belin, D., Carson, M. J. & Beckwith, J. (1995) *J. Bacteriol.* **177,** 4121–4130.
23. Roberts, R. C., Burioni, R. & Helinski, D. R. (1990) *J. Bacteriol.* **172,** 6204–6216.
24. Straight, A. F., Belmont, A. S., Robinett, C. C. & Murray, A. W. (1996) *Curr. Biol.* **6,** 1599–1608.
25. Gietz, R. D. & Sugino, A. (1988) *Gene* **74,** 527–534.
26. Dernburg, A. F. & Sedat, J. W. (1999) *Methods Cell Biol.* **53,** 187–233.
27. Jensen, R. & Shapiro, L. (1999) *Proc. Natl. Acad. Sci. USA* **96,** 10661–10666.
28. Pogliano, J., Osborne, N., Sharp, M. D., Abanes-DeMello, A., Perez, A., Sun, Y.-L. & Pogliano, K. (1999) *Mol. Microbiol.* **31,** 1149–1159.
29. Woldringh, C. L. (1976) *J. Bacteriol.* **125,** 248–257.
30. Webb, C. D., Teleman, A., Gordon, S., Straight, A., Belmont, A., Lin, D. C.-H., Grossman, A. D., Wright, A. & Losick, R. (1997) *Cell* **88,** 667–674.
31. Bignell, C. R., Haines, A. S., Khare, D. & Thomas, C. M. (1999) *Mol. Microbiol.* **34,** 205–216.
32. Durland, R. H. & Helinski, D. R. (1990) *J. Bacteriol.* **172,** 3849–3858.
33. Durland, R. H., Toukdarian, A., Fang, F. & Helinski, D. R. (1990) *J. Bacteriol.* **172,** 3859–3867.
34. Fang, F. C. & Helinski, D. R. (1991) *J. Bacteriol.* **173,** 5861–5868.
35. Figurski, D. H., Meyer, R. J. & Helinski, D. R. (1979) *J. Mol. Biol.* **133,** 295–318.
36. Thomas, C. M., Meyer, R. & Helinski, D. R. (1980) *J. Bacteriol.* **141,** 213–222.
37. Thomas, C. M., Stalker, D. M. & Helinski, D. R. (1981) *Mol. Gen. Genet.* **181,** 1–7.
38. Gerlitz, M., Hrabak, O. & Schwab, H. (1990) *J. Bacteriol.* **172,** 6194–6203.
39. Roberts, R. & Helinski, D. (1992) *J. Bacteriol.* **174,** 8119–8132.
40. Weitao, T., Dasgupta, S. & Nordstrom, K. (2000) *Plasmid* **43,** 200–204.
41. Webb, C. D., Graumann, P. L., Kahana, J. A., Teleman, A. A., Silver, P. A. & Losick, R. (1998) *Mol. Microbiol.* **28,** 883–892.
42. Lin-Chao, S., Chen, W. & Wong, T. (1992) *Mol. Microbiol.* **6,** 3385–3393.
43. Eliasson, A., Bernander, R., Dasgupta, S. & Nordstrom, K. (1992) *Mol. Microbiol.* **6,** 165–170.
44. Niki, H. & Hiraga, S. (1999) *Mol. Microbiol.* **34,** 498–503.